



Cite this: *Phys. Chem. Chem. Phys.*,  
2016, **18**, 12080

# Pressure evolution of the potential barriers of phase transition of MoS<sub>2</sub>, MoSe<sub>2</sub> and MoTe<sub>2</sub>

Xiaofeng Fan,<sup>\*a</sup> David J. Singh,<sup>b</sup> Q. Jiang<sup>a</sup> and W. T. Zheng<sup>a</sup>

Two-dimensional crystals with weak layer interactions, such as twisted graphene, have been a focus of research recently. As a representative example, transitional metal dichalcogenides show a lot of fascinating properties due to stacking orders and spin-orbit coupling. We analyzed the dynamic energy barrier of possible phase transitions in MoX<sub>2</sub> (X = S, Se and Te) with first-principles methods. In the structural transition from 2H<sub>c</sub> to 2H<sub>a</sub>, the energy barrier is found to be increased following an increase of pressure which is different from the phase transition in usual semiconductors. Among MoS<sub>2</sub>, MoSe<sub>2</sub> and MoTe<sub>2</sub>, the energy barrier of MoS<sub>2</sub> is the lowest and the stability of both 2H<sub>c</sub> and 2H<sub>a</sub> is reversed under pressure for MoS<sub>2</sub>. It is found that the absence of a phase transition in MoSe<sub>2</sub> and MoTe<sub>2</sub> is due to the competition between van der Waals interaction of layers and the coulomb interaction of Mo and X in nearest-neighbor layer of Mo in both phases.

Received 1st February 2016,  
Accepted 31st March 2016

DOI: 10.1039/c6cp00715e

www.rsc.org/pccp

## Introduction

Transition metal dichalcogenides, MoX<sub>2</sub> (X = S, Se and Te), as a representative class of 2D layered materials which are readily available and well suited for experimental study, have attracted broad attention due to their rich physical properties and the potential applications in electronic and optoelectronic devices.<sup>1–5</sup> The strong spin-orbit coupling in these materials offers opportunities to study spin-valley coupled 2D physics, such as spin- and valley-Hall effects.<sup>6–10</sup> The weak screening has resulted in tightly bound excitons and strong luminescence from excitons due to the low dimensional limitation.<sup>11–15</sup> Due to strong photoluminescence, and controllable valley and spin polarization, there is a focus on tuning band gaps and addressing the issue of photoluminescence.<sup>16–21</sup> These materials consist of X–Mo–X sheets with these sheets being held together *via* van der Waals (vdW) interaction.<sup>22</sup> Due to the weak interlayer interaction, one of the main uses of MoX<sub>2</sub>, such as MoS<sub>2</sub>, is in dry lubrication. This makes the mechanism of relative slipping between layers interesting.

Unlike graphene with monatomic sp<sup>2</sup> hybridization, the MoS<sub>2</sub> sheets with diatomic layer are coupled to each other by the d-orbital electronic states from Mo. The stacking of layers in different ways leads to the rich polymorphs of MoX<sub>2</sub>, such as 2H<sub>a</sub> and 2H<sub>c</sub>. Under the appropriate conditions, it is possible that there are phase transitions between different structures.<sup>23,24</sup>

Pressure is an effective parameter to analyze changes in structures and electronic properties, amenable to both experimental and theoretical study.<sup>25–29</sup> In prior research, MoS<sub>2</sub> has been found to exhibit a phase transition from 2H<sub>c</sub> to 2H<sub>a</sub>. Under a pressure to 38.8 GPa, Aksoy *et al.* performed an X-ray diffraction study of MoS<sub>2</sub>, identifying a possible transition at about 25 GPa.<sup>30</sup> Later, a 2H<sub>a</sub> phase with space group *P63/mmc* was predicted near 26 GPa.<sup>31,32</sup> The pressure dependence of electronic properties, elastic constants, and structural properties of bulk and few-layer MoS<sub>2</sub> has been investigated theoretically, with the recent experimental analysis of few-layer MoS<sub>2</sub> under pressure.<sup>33–38</sup> Interestingly, it is reported recently that there is no phase transition from 2H<sub>c</sub> to 2H<sub>a</sub> for MoSe<sub>2</sub>.<sup>39</sup> It is possible that the 2H<sub>c</sub> phase is more stable for MoSe<sub>2</sub> under high pressure. The different behavior of MoX<sub>2</sub> under high pressure is an interesting topic. To the best of our knowledge, there is absence of reports about the dynamic processes of phase transitions and structure changes under high pressure for MoX<sub>2</sub>.

In this work, we explore the dynamic processes of the structure changes of MoX<sub>2</sub> under high pressure using first-principles methods. It is found that 2H<sub>c</sub> phase becomes more stable than 2H<sub>a</sub> phase for MoSe<sub>2</sub> and MoTe<sub>2</sub> under pressure, while there is a phase transition for MoS<sub>2</sub>. By analyzing the potential surface, there is a ground state for 2H<sub>c</sub> phase and a local minimum for 2H<sub>a</sub> phase at zero pressure. It is found that the energy barrier from 2H<sub>c</sub> to 2H<sub>a</sub> is increased for all three cases (MoS<sub>2</sub>, MoSe<sub>2</sub> and MoTe<sub>2</sub>), following an increase of pressure. It is considered that the different changes of lattice parameters which are related to the coupling of layers may take an important role in the different behaviors of the three cases.

<sup>a</sup> College of Materials Science and Engineering, Jilin University, Changchun 130012, China. E-mail: xffan@jlu.edu.cn, wtzheng@jlu.edu.cn

<sup>b</sup> Department of Physics and Astronomy, University of Missouri, Columbia, Missouri 65211-7010, USA



## Computational methods

The present calculations are performed within density functional theory using accurate frozen-core full-potential projector augmented-wave (PAW) pseudopotentials, as implemented in the VASP code.<sup>40,41</sup> We did calculations with the generalized gradient approximation (GGA) of Perdew, Burke and Ernzerhof (PBE) and with added vdW corrections.<sup>42</sup> The plane-wave basis sets and  $k$ -space integrals are chosen to ensure that the total energy is converged at 1 meV per atom level. A kinetic energy cutoff of 500 eV for the plane wave expansion is found to be sufficient. The Brillouin zones are sampled with dense  $\Gamma$ -centered  $16 \times 16 \times 4$  grids. The effect of dispersion interaction is included by the empirical correction scheme of Grimme (DFT + D/PBE).<sup>43</sup> This approach has been successful in describing layered structures.

The calculated lattice constants  $a$  and  $c$  of bulk  $\text{MoS}_2$  are 3.192 Å and 12.465 Å. For  $\text{MoSe}_2$  and  $\text{MoTe}_2$ , the lattice parameters  $a$  and  $c$  are 3.319 Å and 13.113 Å, 3.526 Å and 14.162 Å, respectively. These are all similar to the experimental values for  $\text{MoS}_2$ ,  $\text{MoSe}_2$  and  $\text{MoTe}_2$ . The small overestimate of the lattice constants with the PBE functional is not significant for our analysis about the effects of pressure on the structural transition. The method for applying pressure in the present calculations was to add external stress to stress tensor in VASP code,<sup>41</sup> and the structures of bulk  $\text{MoX}_2$  with different phases were then optimized under the specified hydrostatic pressure. The added external stress is isotropic and compressive to simulate the real conditions in experiments. We analyzed the energy barriers for transformations between the different phases for pressures up to 28 GPa. It may be noticed that there is Pulay stress in the calculations due to the incompleteness of the plane wave basis set. With the proper plane wave basis set, the small Pulay stress can be ignored in the large range of pressure (0–28 GPa) in this work.

## Results and discussion

### Phase transition of $\text{MoX}_2$ under pressure

As a result of the different ways of stacking of layers, there are two well-known phases,  $2H_c$  and  $2H_a$ , with hexagonal symmetry.

The  $2H_c$  phase is of  $P63/mmc$  space group and  $2H_a$  has the same space group. The difference of both phases is due to the relative plane slipping between the nearest-neighbor layers. In the hexagonal plane of the unit cell, there are three special sites which can be occupied by Mo, namely sites a (0, 0), b ( $1/3$ ,  $2/3$ ) and c ( $2/3$ ,  $1/3$ ). In the kind of  $2H$  structures, there are two layers of Mo in one unit cell and each layer has hexagonal symmetry with space group  $P\bar{6}m2$ . Therefore, there are just two stacking ways for Mo double layers which are topologically different, such as  $aa$  and  $ab$  stacking which result in the  $2H_a$  and  $2H_c$  phase (in Fig. 1a), respectively. At zero pressure, it is found that  $2H_c$  phase is more stable than  $2H_a$  phase for all three cases:  $\text{MoS}_2$ ,  $\text{MoSe}_2$  and  $\text{MoTe}_2$ .

We calculated the energies of  $2H_c$  and  $2H_a$  phases for three cases under different pressures. In the calculation, the added vdW interaction, which is found to be important for the interlayer interactions even at high pressure, is considered. In Fig. 1b, we show the change of enthalpy following an increase of pressure. It should be noticed that the contributions of zero-point energy and entropy are ignored, since both phases are very similar from the local chemical bonding point of view. The enthalpy difference between  $2H_c$  and  $2H_a$  changes substantially with pressure and the trend is obviously different for the three cases (Fig. 1b). Up to 28 GPa, the relative enthalpy of  $\text{MoTe}_2$  increases with pressure and that of  $\text{MoSe}_2$  does not change obviously. For  $\text{MoS}_2$ , there is a phase transition at about 13 GPa. These results are consistent with the recent report about the experimental observation of  $2H_a$  phase of  $\text{MoS}_2$  under high pressure and the absence of a phase transition for  $\text{MoSe}_2$  under high pressure.<sup>27,28,39</sup>

### Energy surface, pathway and energy barrier

In the unit cell of  $2H_c$  phase, the second layer of  $\text{MoX}_2$  is stacked with a rotation of  $60^\circ$  along the  $z$  axis relative to the first layer which is one of two basic types of stacking ways. Another one is where there is no rotation between nearest-neighbor  $\text{MoX}_2$  layers which forms the basis of  $3R$ -type  $\text{MoX}_2$ . Usually, the rotation between nearest-neighbor layers with vdW interactions is more difficult than the relative plane slipping between layers due to the higher energy barrier which the rotation needs

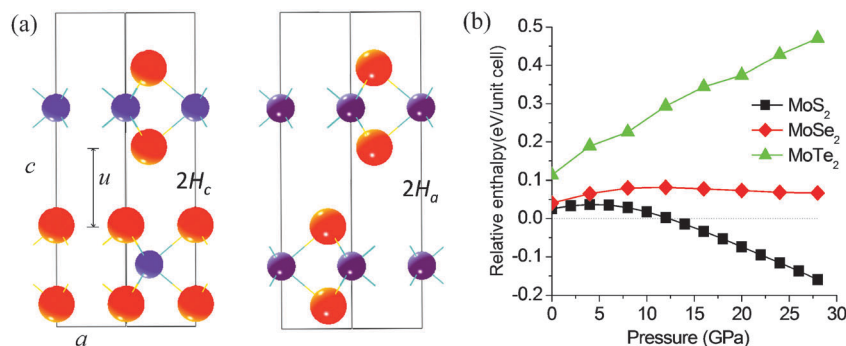


Fig. 1 Structures of both phases  $2H_c$  and  $2H_a$  of hexagonal AB-stacking  $\text{MoX}_2$  ( $X = \text{S}, \text{Se}$  and  $\text{Te}$ ) (a) and relative enthalpies of  $2H_c$  and  $2H_a$  as a function of pressure for  $\text{MoS}_2$ ,  $\text{MoSe}_2$  and  $\text{MoTe}_2$  (b). Note that the enthalpy of  $2H_a$   $\text{MoX}_2$  is defined to be zero for each pressure.



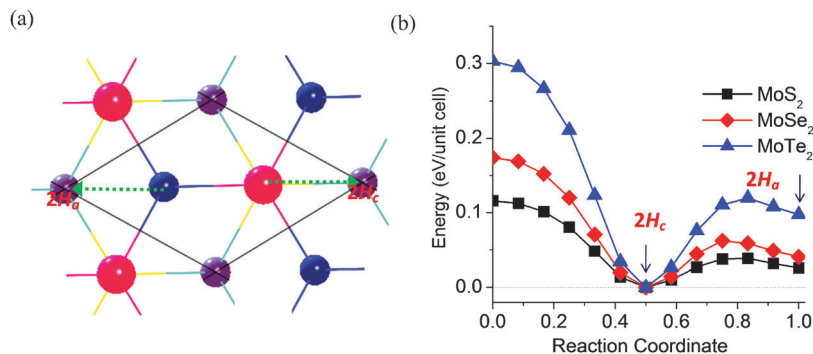


Fig. 2 Schematic representation of the relative plane sliding between two  $\text{MoX}_2$  ( $X = \text{S}, \text{Se}$  and  $\text{Te}$ ) layers for a unit cell of hexagonal  $\text{MoX}_2$  with 2-layer structure by AB stacking (a), and the variation of total energy per unit cell along the path indicated by the arrow in (a) under zero pressure (b). Note that the structure becomes  $2\text{H}_a$  phase if the Mo atom of the second layer indicated in (a) moves to the site labeled “ $2\text{H}_a$ ”, and becomes  $2\text{H}_c$  phase if the X atom of the second layer indicated in (a) moves to the site labeled “ $2\text{H}_c$ ”.

to go through. Under pressure, the layers with weak interaction slip more easily relative to each other.

For single-layer  $\text{MoX}_2$  with 2H-type structure, there is rotational symmetry of  $C_3$  along the  $z$ -axis. Therefore, in the case of the way of layer stacking to which  $2\text{H}_c$  and  $2\text{H}_a$  phases belong, there are two kinds of pathways with high symmetry, as shown in Fig. 2a. For each kind of pathway, there are three pathways which is equivalent with  $C_3$  symmetry. We simulated the energy surfaces along the two kinds of pathways for  $\text{MoS}_2$ ,  $\text{MoSe}_2$  and  $\text{MoTe}_2$  in Fig. 2b. It can be found that there are two local energy minima in the surface including the ground state and metastable state. Actually, the two states are corresponding to  $2\text{H}_c$  and  $2\text{H}_a$  phases, respectively. Around the two local minima, there is an energy barrier on both sides which is about 0.3 eV per unit cell relative to the ground state  $2\text{H}_c$ . The energies of  $2\text{H}_a$  phase are about 26, 41 and 97 meV per unit cell higher than those of  $2\text{H}_c$  for  $\text{MoS}_2$ ,  $\text{MoSe}_2$  and  $\text{MoTe}_2$ , respectively. The barrier from  $2\text{H}_c$  to  $2\text{H}_a$  is 38.8, 62.2 and 119.8 meV per unit cell for the three cases, respectively. Therefore, if there is a phase transition between  $2\text{H}_c$  and  $2\text{H}_a$ , it is easier for  $\text{MoS}_2$  than for  $\text{MoSe}_2$  and  $\text{MoTe}_2$ .

Phase transition between  $2\text{H}_c$  and  $2\text{H}_a$  is different from the usual structural transition in which there are breaking and re-bonding of chemical bonds. For the layered  $\text{MoX}_2$ , it is just the relative slipping in response to the possible phase transition under weak perturbation, such as when the pressure is not very high. To simulate the phase transition of  $\text{MoX}_2$  under pressure, an expanded nudged elastic band method is adopted by building the potential reaction path with a series of intermediate images and relaxing the structures of the intermediate images. The internal coordinate of Mo atom of the first layer in the unit cell is fixed. A series of points along the pathway from  $2\text{H}_a$  to  $2\text{H}_c$  is set for the atomic coordinates of the second layer. For some point of the pathway, the internal coordinate of Mo atom of the second layer is fixed. Then the parameters of the whole cell including the lattice parameters need to be relaxed under the fixed pressure while the internal coordinates of other atoms are also relaxed in the unit cell. From these processes, we can obtain the enthalpies of a series of structures along the pathway at the fixed pressure.

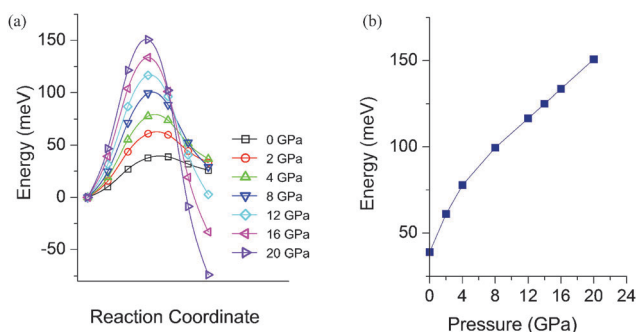


Fig. 3 Variation of enthalpy from the layered structure  $2\text{H}_c$   $\text{MoS}_2$  to  $2\text{H}_a$   $\text{MoS}_2$  following the pathway of plane sliding indicated in Fig. 2a for different pressures (a) and energy barrier as a function of the pressure calculated by PBE/GGA with dispersion interactions (b). Note that the total energy is given relative to the total energy of  $2\text{H}_c$   $\text{MoS}_2$  at zero pressure and the barrier energy is calculated with a unit cell of double-layer  $\text{MoS}_2$ .

In Fig. 3a, we plot the change of enthalpy along the pathway from  $2\text{H}_c$  to  $2\text{H}_a$  for  $\text{MoS}_2$  under different pressures. It is obvious that  $2\text{H}_a$  becomes more stable than  $2\text{H}_c$  with an increase of pressure. In Fig. 3b, the energy barrier from  $2\text{H}_c$  to  $2\text{H}_a$  following a change of pressure is plotted. The barrier has a trend of increasing with an increase of pressure. It is different from the usual structural transition in which the barrier decreases following an increase of pressure, such as the phase transition of BN from low-density phase to low-energy phase.<sup>26</sup> At 13 GPa, the energy barrier for the phase transition from  $2\text{H}_c$  to  $2\text{H}_a$  is about 120 meV per unit cell. Fortunately, the barrier is not so high, from this theoretical analysis. This may be the reason that the phase transition is observed in  $\text{MoS}_2$ . For deducing the increase of barriers under pressure, one may perform experiments about phase transitions of  $\text{MoS}_2$  with pressure under different temperatures.

In Fig. 4a and 5a, the changes of enthalpies along the pathway are plotted for  $\text{MoSe}_2$  and  $\text{MoTe}_2$ .  $2\text{H}_a$  phase does not become more stable than  $2\text{H}_c$ . In addition, the energy barrier from  $2\text{H}_c$  to  $2\text{H}_a$  is increased following an increase of pressure, as shown in Fig. 4b and 5b. Interestingly, among the



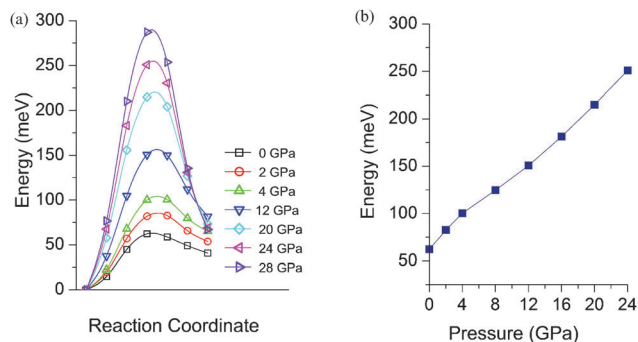


Fig. 4 Variation of enthalpy from the layered structure  $2H_c$  MoSe<sub>2</sub> to  $2H_a$  MoSe<sub>2</sub> following the pathway of plane sliding indicated in Fig. 2a for different pressures (a) and energy barrier as a function of the pressure calculated by PBE/GGA with dispersion interactions (b). Note that the total energy is given relative to the total energy of  $2H_c$  MoSe<sub>2</sub> at zero pressure and the barrier energy is calculated with a unit cell of double-layer MoSe<sub>2</sub>.

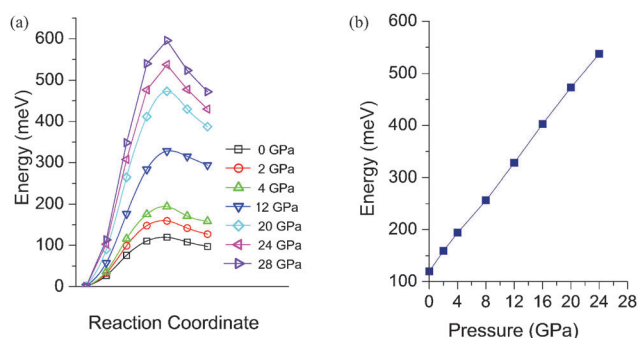


Fig. 5 Variation of enthalpy from the layered structure  $2H_c$  MoTe<sub>2</sub> to  $2H_a$  MoTe<sub>2</sub> following the pathway of plane sliding indicated in Fig. 2a for different pressures (a) and energy barrier as a function of the pressure calculated by PBE/GGA with dispersion interactions (b). Note that the total energy is given relative to the total energy of  $2H_c$  MoTe<sub>2</sub> at zero pressure and the barrier energy is calculated with a unit cell of double-layer MoTe<sub>2</sub>.

change of energy barrier of the three cases under pressure, the increase of MoTe<sub>2</sub> is the fastest one and that of MoS<sub>2</sub> is the slowest one. This may be due to the largest p orbitals of Te among the three cases. In the processes from  $2H_c$  to  $2H_a$ , the X atom of the second layer needs to go through the middle of two nearest-neighbor X atoms of the first layer which corresponds

to the configuration of the energy barrier. Therefore, with increasing pressure, the shorter distance between layers leads to the increase of the barrier. The larger p orbitals of X atoms also results in the increase of the barrier.

From the above results, the phase transition happens only in MoS<sub>2</sub> due to a slip between layers and not in MoSe<sub>2</sub> and MoTe<sub>2</sub>. Intuitively, it would be more difficult in MoS<sub>2</sub>, where S is very reactive and the lattice constant is small. The main reason is the p orbitals of X are hybridized with the d orbitals of Mo and the charge transfer from Mo to S makes the S ion more negative than Se and Te in MoSe<sub>2</sub> and MoTe<sub>2</sub>. The coulomb interaction between S ions from different layers is repulsive. Even under a pressure of 28 PGa, the distance between S ions from nearest-neighbor MoS<sub>2</sub> layers is 2.83 Å in  $2H_c$  phase (2.67 Å in  $2H_a$  phase) and is larger than the bond length of S–S bond (2.05 Å). The repulsive interaction between S ions from different layers makes the slip between layers easy. In MoSe<sub>2</sub> and MoTe<sub>2</sub>, the phenomenon is similar to that in MoS<sub>2</sub>. In MoSe<sub>2</sub>, the distance between Se ions from nearest-neighbor layers under 28 GPa is 2.96 Å in  $2H_c$  (2.86 Å in  $2H_a$ ) and is larger than the bond length of Se–Se bond (2.29 Å). In MoTe<sub>2</sub>, the distance between Te ions from nearest-neighbor layers under 28 GPa is 3.15 Å in  $2H_c$  (3.10 Å in  $2H_a$ ) and is larger than the bond length of Se–Se bond (2.64 Å).

### Structural changes under high pressure

Following an increase of pressure, the lattice constants and volumes of both  $2H_a$  and  $2H_c$  are decreased for the three cases, as is known. The decrease of lattice parameter  $c$  for both phases is faster than that of parameter  $a$ . This can be attributed to the weak interaction between layers. Under pressure, the parameter  $u$  which indicates the distance between layers has a similar trend to that of parameter  $c$ . It is noticed that the parameters  $c$  and  $u$  of  $2H_a$  are larger than those of  $2H_c$  for the three cases at zero pressure. This may be the reason that the  $2H_c$  phase is more stable than  $2H_a$  for the three cases.

With an increase of pressure, the parameters  $c$  and  $u$  of  $2H_a$  become smaller than those of  $2H_c$ , as shown in Fig. 6. From rough evaluation, the vdW interaction between layers will increase following the decrease of layer distance. This means it is possible that  $2H_a$  is more stable than  $2H_c$  with an increase of pressure and there will be a possible phase transition for

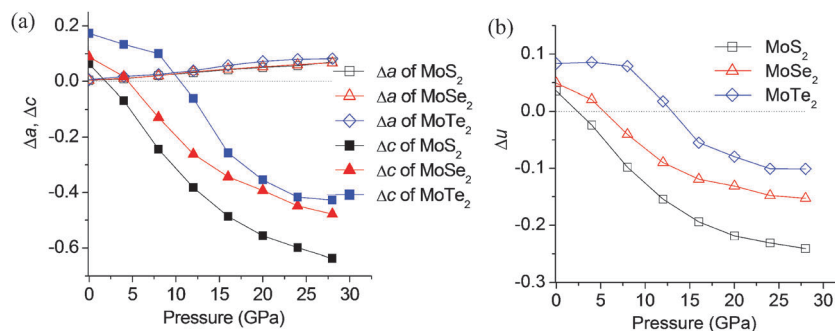


Fig. 6 Difference between lattice constants ( $a$  and  $c$ ) of  $2H_a$  and of  $2H_c$  ( $\Delta a = a(2H_a) - a(2H_c)$ ,  $\Delta c = c(2H_a) - c(2H_c)$ ) as a function of pressure (a) and difference between lattice parameter  $u$  (defined in Fig. 1a) of  $2H_a$  and of  $2H_c$  ( $\Delta u = u(2H_a) - u(2H_c)$ ) as a function of pressure for MoX<sub>2</sub> (X = S, Se and Te).



MoS<sub>2</sub>, MoSe<sub>2</sub> and MoTe<sub>2</sub>. However, the phase transition only happens for MoS<sub>2</sub>. This may be attributed to another effect in that the coulomb interaction between Mo of one layer and X of nearest-neighbor layer in 2H<sub>c</sub> structure is stronger than that in 2H<sub>a</sub> structure, due to the shorter distance between Mo and X in two layers for 2H<sub>c</sub> phase under pressure. Therefore, both effects (vdW and coulomb interactions) compete with each other, following an increase of pressure. In the three cases, the changes of parameters  $\Delta c$  and  $\Delta u$  of MoS<sub>2</sub> under pressure are the largest ones. This may mean that the vdW interaction of 2H<sub>a</sub> MoS<sub>2</sub> is the strongest and the 2H<sub>a</sub> phase of MoS<sub>2</sub> becomes more stable than 2H<sub>c</sub> under pressure.

## Conclusions

With the first-principles method, we studied the dynamic processes of phase transitions of MoX<sub>2</sub> (X = S, Se and Te). The calculation results show that MoS<sub>2</sub> has a phase transition and the phase transition in MoSe<sub>2</sub> and MoTe<sub>2</sub> is absent under pressure and are consistent with the recent experimental observation in MoS<sub>2</sub> and MoSe<sub>2</sub>. For the structural transition from 2H<sub>c</sub> to 2H<sub>a</sub> in MoX<sub>2</sub>, the dynamic energy barrier is increased following an increase of pressure. This is attributed to the decrease of layer distance. Among MoS<sub>2</sub>, MoSe<sub>2</sub> and MoTe<sub>2</sub>, the energy barrier of MoS<sub>2</sub> is the lowest due to the small p orbitals of S compared to those of Se and Te. The absence of phase transition in MoSe<sub>2</sub> and MoTe<sub>2</sub> is attributed to the competition between vdW and coulomb interactions. The transition from semiconductor to metallic conductor in MoX<sub>2</sub> under pressure is due to the strong coupling of layers and is not related to the structural phase transition from 2H<sub>c</sub> to 2H<sub>a</sub>.

## Acknowledgements

The support from the National Natural Science Foundation of China (no. 11504123) is highly appreciated. Work at the University of Missouri was supported by the Department of Energy, BES through the MAGICs center.

## References

- 1 K. F. Mak, C. Lee, J. Hone, J. Shan and T. F. Heinz, Atomically Thin MoS<sub>2</sub>: A New Direct-Gap Semiconductor, *Phys. Rev. Lett.*, 2010, **105**, 136805.
- 2 B. Radisavljevic, A. Radenovic, J. Brivio, V. Giacometti and A. Kis, Single-Layer MoS<sub>2</sub> Transistors, *Nat. Nanotechnol.*, 2011, **6**, 147–150.
- 3 Q. H. Wang, K. Kalantar-Zadeh, A. Kis, J. N. Coleman and M. S. Strano, Electronics and Optoelectronics of Two-Dimensional Transition Metal Dichalcogenides, *Nat. Nanotechnol.*, 2012, **7**, 699–712.
- 4 C. Lee, *et al.*, Anomalous lattice vibrations of single- and few-layer MoS<sub>2</sub>, *ACS Nano*, 2010, **4**, 2695–2700.
- 5 A. Splendiani, *et al.*, Emerging Photoluminescence in Monolayer MoS<sub>2</sub>, *Nano Lett.*, 2010, **10**, 1271–1275.
- 6 Y. Zhang, *et al.*, Direct observation of the transition from indirect to direct bandgap in atomically thin epitaxial MoSe<sub>2</sub>, *Nat. Nanotechnol.*, 2014, **9**, 111–115.
- 7 P.-C. Yeh, *et al.*, Layer-dependent electronic structure of an atomically heavy two-dimensional dichalcogenide, *Phys. Rev. B: Condens. Matter Mater. Phys.*, 2015, **91**, 041407.
- 8 H. Zeng, J. Dai, W. Yao, D. Xiao and X. Cui, Valley polarization in MoS<sub>2</sub> monolayers by optical pumping, *Nat. Nanotechnol.*, 2012, **7**, 490–493.
- 9 T. Cao, *et al.*, Valley-selective circular dichroism of monolayer molybdenum disulphide, *Nat. Commun.*, 2012, **3**, 887.
- 10 D. Xiao, G.-B. Liu, W. Feng, X. Xu and W. Yao, Coupled Spin and Valley Physics in Monolayers of MoS<sub>2</sub> and Other Group-VI Dichalcogenides, *Phys. Rev. Lett.*, 2012, **108**, 196802.
- 11 A. R. Klots, *et al.*, Probing excitonic states in suspended two-dimensional semiconductors by photocurrent spectroscopy, *Sci. Rep.*, 2014, **4**, 6608.
- 12 X. Li, F. Zhang and Q. Niu, Unconventional quantum Hall effect and tunable spin Hall effect in Dirac materials: application to an isolated MoS<sub>2</sub> trilayer, *Phys. Rev. Lett.*, 2013, **110**, 066803.
- 13 J. S. Ross, *et al.*, Electrical control of neutral and charged excitons in a monolayer semiconductor, *Nat. Commun.*, 2013, **4**, 1474.
- 14 K. F. Mak, *et al.*, Tightly bound trions in monolayer MoS<sub>2</sub>, *Nat. Mater.*, 2013, **12**, 207–211.
- 15 K. F. Mak, K. L. McGill, J. Park and P. L. McEuen, The valley Hall effect in MoS<sub>2</sub> transistors, *Science*, 2014, **344**, 1489–1492.
- 16 J. Feng, X. Qian, C.-W. Huang and J. Li, Strain-Engineered Artificial Atom as a Broad-Spectrum Solar Energy Funnel, *Nat. Photonics*, 2012, **6**, 866–872.
- 17 C.-H. Chang, X. Fan, S.-H. Lin and J.-L. Kuo, Orbital analysis of electronic structure and phonon dispersion in MoS<sub>2</sub>, MoSe<sub>2</sub>, WS<sub>2</sub>, and WSe<sub>2</sub> monolayers under strain, *Phys. Rev. B: Condens. Matter Mater. Phys.*, 2013, **88**, 195420.
- 18 S. Mouri, Y. Miyauchi and K. Matsuda, Tunable photoluminescence of monolayer MoS<sub>2</sub> via chemical doping, *Nano Lett.*, 2013, 5944–5948.
- 19 S. Tongay, *et al.*, Defects activated photoluminescence in two-dimensional semiconductors: interplay between bound, charged, and free excitons, *Sci. Rep.*, 2013, **3**, 2657.
- 20 E. Scalise, M. Houssa, G. Pourtois, V. Afanasev and A. Stesmans, Strain-induced semiconductor to metal transition in the two-dimensional honeycomb structure of MoS<sub>2</sub>, *Nano Res.*, 2012, **5**, 43–48.
- 21 H. J. Conley, *et al.*, Bandgap Engineering of Strained Monolayer and Bilayer MoS<sub>2</sub>, *Nano Lett.*, 2013, **13**, 3626–3630.
- 22 A. K. Geim and I. V. Grigorieva, Van der Waals heterostructures, *Nature*, 2013, **499**, 419–425.
- 23 Y.-C. Lin, D. O. Dumcenco, Y.-S. Huang and K. Suenaga, Atomic mechanism of the semiconducting-to-metallic phase transition in single-layered MoS<sub>2</sub>, *Nat. Nanotechnol.*, 2014, **9**, 391–396.
- 24 H. H. Huang, *et al.*, Controlling phase transition for single-layer MTe<sub>2</sub> (M = Mo and W): modulation of the potential



- barrier under strain, *Phys. Chem. Chem. Phys.*, 2016, **18**, 4086–4094.
- 25 A. W. Webb, *et al.*, High Pressure Investigations of MoS<sub>2</sub>, *J. Phys. Chem. Solids*, 1976, **37**, 329.
- 26 X. Fan, W. T. Zheng, Q. Jiang and D. J. Singh, Pressure evolution of the potential barriers for transformations of layered BN to dense structures, *RSC Adv.*, 2015, **5**, 87550–87555.
- 27 A. P. Nayak, *et al.*, Pressure-induced semiconducting to metallic transition in multilayered molybdenum disulfide, *Nat. Commun.*, 2014, **5**, 3731.
- 28 Z.-H. Chi, *et al.*, Pressure-Induced Metallization of Molybdenum Disulfide, *Phys. Rev. Lett.*, 2014, **113**, 036802.
- 29 G. Eda, *et al.* Photoluminescence from chemically exfoliated MoS<sub>2</sub>, *Nano Lett.*, 2011, **11**, 5111.
- 30 R. Aksoy, *et al.*, X-ray Diffraction Study of Molybdenum Disulfide to 38.8 GPa, *J. Phys. Chem. Solids*, 2006, **67**, 1914.
- 31 L. Hromadova, R. Martonak and E. Tosatti, Structure Change, Layer Sliding, and Metallization in High-pressure MoS<sub>2</sub>, *Phys. Rev. B: Condens. Matter Mater. Phys.*, 2013, **87**, 144105.
- 32 N. Bandaru, *et al.*, Effect of Pressure and Temperature on Structural Stability of MoS<sub>2</sub>, *J. Phys. Chem. C*, 2014, **118**, 3230–3235.
- 33 X. Dou, K. Ding, D. Jiang and B. Sun, Tuning and Identification of Interband Transitions in Monolayer and Bilayer Molybdenum Disulfide Using Hydrostatic Pressure, *ACS Nano*, 2014, **8**, 7458.
- 34 X. Fan, C. H. Chang, W. T. Zheng, J.-L. Kuo and D. J. Singh, The Electronic Properties of Single-Layer and Multilayer MoS<sub>2</sub> under High Pressure, *J. Phys. Chem. C*, 2015, **119**, 10189–10196.
- 35 X. Dou, K. Ding, D. Jiang, X. Fan and B. Sun, Probing Spin–Orbit Coupling and Interlayer Coupling in Atomically Thin Molybdenum Disulfide Using Hydrostatic Pressure, *ACS Nano*, 2016, **10**, 1619–1624.
- 36 H. Peelaers and C. G. Van de Walle, Elastic Constants and Pressure-Induced Effects in MoS<sub>2</sub>, *J. Phys. Chem. C*, 2014, **118**, 12073–12076.
- 37 H. Guo, T. Yang, P. Tao, Y. Wang and Z. Zhang, High Pressure Effect on Structure, Electronic Structure, and Thermoelectric Properties of MoS<sub>2</sub>, *J. Appl. Phys.*, 2013, **113**, 013709.
- 38 M. Rifliková, R. Martoňák and E. Tosatti, Pressure-induced gap closing and metallization of MoSe<sub>2</sub> and MoS<sub>2</sub>, *Phys. Rev. B: Condens. Matter Mater. Phys.*, 2014, **90**, 035108.
- 39 Z. Zhao, *et al.* Pressure induced metallization with absence of structural transition in layered molybdenum diselenide, *Nat. Commun.*, 2014, **6**, 7312.
- 40 G. Kresse and J. Furthmüller, Efficient Iterative Schemes for Ab Initio Total-Energy Calculations Using a Plane-wave Basis Set, *Phys. Rev. B: Condens. Matter Mater. Phys.*, 1996, **54**, 11169–11186.
- 41 G. Kresse and J. Furthmüller, Efficiency of Ab Initio Total Energy Calculations for Metals and Semiconductors Using a Plane-wave Basis Set, *Comput. Mater. Sci.*, 1996, **6**, 15–50.
- 42 J. P. Perdew, K. Burke and M. Ernzerhof, Generalized Gradient Approximation Made Simple, *Phys. Rev. Lett.*, 1996, **77**, 3865–3868.
- 43 S. Grimme, Semiempirical GGA-Type Density Functional Constructed with a Long-Range Dispersion Correction, *J. Comput. Chem.*, 2006, **27**, 1787.

